Continuous monitoring of a challenging heritage tower in Monza, Italy

Antonella Saisi[1,2] · Carmelo Gentile[1,2] · Antonello Ruccolo[1,2]

Abstract
A recent survey of the historic complex of "Santa Maria del Carrobiolo" in Monza (Italy) highlighted that two sides of the bell-tower are directly supported by the load-bearing walls of the apse and South aisle of the neighbouring church. After the discovery of the weak structural arrangement of the building, a network of 10 displacement transducers, integrated by five temperature sensors, was installed in the tower to check the opening variation of the main cracks. Subsequently, ambient vibration tests were performed and closely spaced modes with similar mode shapes were clearly identified: since the dynamic characteristics of the tower are quite different from those obtained in past experimental studies of similar structures and conceivably related to the construction sequence, a simple dynamic monitoring system was installed in the tower to complete the health monitoring aimed at the preservation of the historic structure. The paper—after a brief description of the tower and a summary of selected evidences provided by on-site survey, historic research and static monitoring—focuses on the dynamic characteristics identified in the preliminary ambient vibration tests and the main results of 1-year dynamic monitoring. In order to assess the effects of changing temperature on the natural frequencies of the investigated tower, especially in view of the removal of those effects needed for an effective performance assessment, simple correlation studies between modal frequencies and temperature are presented and discussed.

Keywords Architectural heritage · Automated modal identification · Closely spaced modes · Environmental effects · Frequency crossing/veering · Masonry towers

1 Introduction

Masonry towers are very common cultural heritage buildings in Italy, where churches and bell-towers were built even in smaller towns and a large number of defensive towers and chimneys dates back to Middle Age and the Industrial Revolution period, respectively. Ancient towers are usually slender and subjected to significant dead loads, so that those structures often exhibit high vulnerability to seismic actions, as it has been dramatically testified also by the recent Italian events, such as the ones hitting the Emilia region in 2012 [1] and the Central Italy in 2016 [2].

✉ Carmelo Gentile
carmelo.gentile@polimi.it

[1] Politecnico di Milano, Milan, Italy

[2] Department of Architecture, Built environment and Construction engineering (ABC), Piazza Leonardo da Vinci, 32, 20133 Milan, Italy

Since towers are generally sensitive also to ambient excitation, such as micro-tremors and wind, dynamic tests in operational conditions are becoming more popular as assessment tools (see e.g. [3] for a list of recent studies reported in the literature). Furthermore, historic towers exhibit a cantilever-like dynamic behaviour, so that the successful monitoring of the dynamic characteristics of the structure can be obtained through automated operational modal analysis (OMA) [4–7] of the data continuously collected by a few high-sensitivity accelerometers, which are permanently installed in the upper part of the building [8–14]. Hence, the idea of implementing vibration-based and cost-effective Structural Health Monitoring (SHM, i.e. the continuous interrogation of sensors installed in the structure aimed at extracting features which are representative of the current state of structural health) for the condition-based maintenance of historic towers has been taking shape recently.

Indeed, the possibility of using a limited number of accelerometers in the SHM of ancient towers is especially promising to promote extensive and sustainable

This is a post-peer-review, pre-copyedit version of an article published in Journal of Civil Structural Health Monitoring, 2018, 8:1, 77-90. The final authenticated version is available online at: http://dx.doi.org/10.1007%2Fs13349-017-0260-5

programmes of condition-based maintenance but often implies the choice of natural frequencies as sensitive features for anomaly detection. On the other hand, natural frequencies are also sensitive to factors other than structural changes—such as the environmental and the operational conditions [15]—and especially the temperature turned out to be a dominant driver of modal frequency changes in masonry towers [8–14], so that an effective approach to SHM should include the removal (or minimization) of the temperature effects on identified natural frequencies.

The paper mainly focuses on the results of the continuous dynamic monitoring programme performed on the bell-tower belonging to the historic complex of "Santa Maria del Carrobiolo" in Monza, Italy [16, 17]. The complex of religious buildings includes a church, a bell-tower, a monastery and several other buildings. Based on historical documents [16], the church and monastery were built before than the bell-tower.

The dynamic monitoring of the bell-tower follows a pre-diagnostic survey [17], recently carried out within a survey programme of the main worship buildings in Monza. Direct survey of the masonry discontinuities confirmed that the tower was built after the church and revealed that two sides of the bell-tower are directly supported by the load-bearing walls of the church apse and the last part of right aisle. The construction sequence adopted for the tower, not identified before, raised obvious concern about the performance of the structure under wind and seismic actions. Therefore, a wide research programme was planned to assess the structural condition of the building and is currently in progress. In more details, the research consists of the fol-lowing steps: (a) prompt on-site investigation, including geometric survey and visual inspections; (b) static moni-toring of the main cracks through the installation of 10 displacement transducers (as well as five temperature sensors) at different levels of the tower; (c) ambient vibration testing and identification of the dynamic char-acteristics of the tower using OMA; (d) installation of a simple dynamic monitoring system in the tower.

After a brief description of the bell-tower, the paper presents some evidences provided by the static monitoring (Sect. 2), aimed at highlighting some distinctive features of the investigated structure. Subsequently, the dynamic monitoring is addressed and full details are given on preliminary ambient vibration tests (Sect. 3), the monitoring hardware and the procedures adopted to automatically identify the modal parameters from continuously collected data (Sect. 4). At last (Sect. 5), the main results of 1-year dynamic monitoring and the correlation between natural frequencies and environmental factors are presented and discussed.

2 Description of the bell-tower and static monitoring

The historic complex of "Santa Maria del Carrobiolo" in Monza (Italy) [16] was originally built by the Italian religious order known as Humiliati suppressed in 1571 by Pope Pio V and passed to the Barnabite order in 1574. The religious complex includes a church, a bell-tower, a monastery, an oratory and other minor buildings, which were erected at different times. The tower (Fig. 1), about 33.7 m high, is built in solid brick masonry and has nearly square plan (5.93 m $\times$ 5.70 m); the thickness of the load-bearing walls slightly decreases from 70 cm at the ground level to 58 cm at the top.

The documentary research indicated that the construction of the church and the monastery dates back to thirteenth century, whereas a date engraved on a stone of the bell-tower traces the likely conclusion of its construction back to 1339 [16]. Direct survey of the masonry discontinuities provided clear evidence of the construction sequence and revealed that two sides of the tower are directly supported by the load-bearing walls of the church apse and the last part of South aisle (Fig. 2). Moreover, the load-bearing walls of the tower (East and South side) are just leant against the existing walls of the church and the discontinuities due to the building phases look very sharp, confirming the lack of connection between the different parts.

Above the church height, the masonry texture seems homogeneous, even if several cracks are present (Figs. 1b and 3). Major cracks are visible indoor in the centre of both East and West fronts of the tower. Other important cracks, cutting the entire wall thickness, are concentrated at the level below the belfry and diffused on all the sides, across the large windows. It should be noticed that (Fig. 4) the opening of a deep crack on the West side is opposed by the presence of one metallic tie-rod.

The detection of the weak structural arrangement of the tower resulting from the construction sequence caused growing concern about the actual structural performance. In addition, a few months before the pre-diagnostic survey, the construction of an under-ground car park adjacent to the bell-tower increased the movement of the pre-existing cracks and the sharp discontinuities related to the construction phases: at the base of the tower, some cracks appeared on the plaster after a recent wall painting. The re-opening of cracks already repaired suggested to setup a static monitoring system.

The static monitoring system was installed on June 2014, according to the general layout schematically shown in Fig. 5, and consists of a network of 10 displacement transducers, integrated by five temperature sensors. The

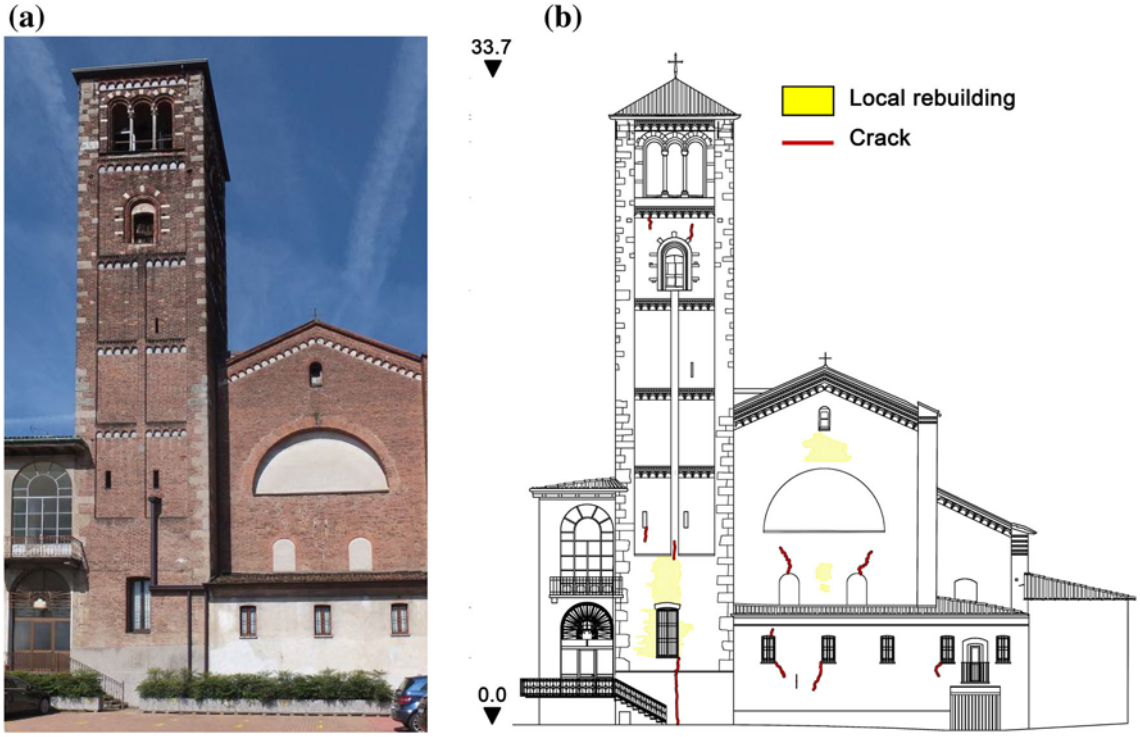

Fig. 1 The church of the *Santa Maria del Carrobiolo* and the bell-tower (Monza, Italy): **a** East view; **b** geometric survey of the East front (dimensions in m)

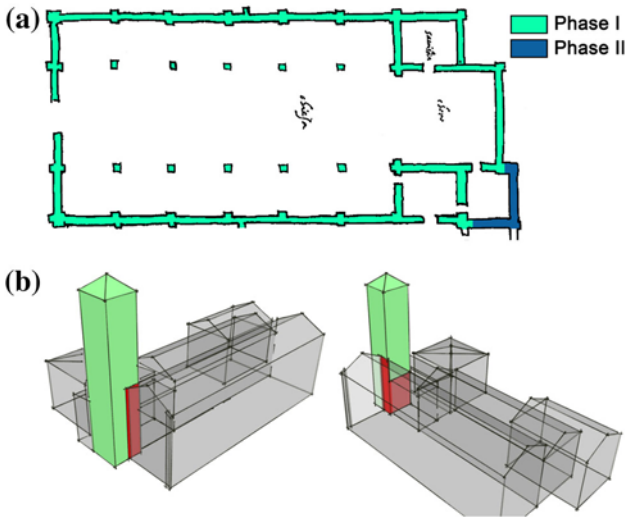

Fig. 2 **a** Building phases in a plan dating back to 1572; **b** schematic representation of the interaction between the bell-tower and the church apse

displacement transducers (Fig. 6a), installed on the main cracks and discontinuities, are linear sensors (potentiometers) with a maximum stroke of 25 mm and a maximum error on the linearity of 0.2%.

It is worth mentioning that: (a) displacements and temperatures are automatically collected every 10 min; (b) the displacement transducers denoted as 1–2, 3–4 and 5–8 in Fig. 5 are placed inside the tower in order to check the opening of the main cracks at Level 0, Level 1 and Level 2, respectively; (c) the last couple of sensors (9–10 in Fig. 5) is installed on the South wall of the church, in the close vicinity of the tower; (d) each couple of displacement transducers, along with one temperature sensor, is connected to one data logger for the automatic data acquisition and wireless transmission to a master unit equipped with a GSM-GPRS modem. It is further noticed that the temperature sensors belonging to the static monitoring system—denoted as T_{0N}, T_{1E}, T_{2E}, T_{2W} and T_S in Fig. 5—allow to measure both the indoor temperature at different levels of the tower and the outdoor temperature on the South side of the structure; hence, a relatively dense representation of the temperature conditions of the tower is achieved.

As previously pointed out, one metallic tie-rod (Fig. 4) is placed above a main crack of the West side, which is surveyed by the transducer TL2_SOCH2 (Fig. 6b).

Figure 7a reports the time evolution of the outdoor temperature T_S, the indoor temperature T_{0N} and the displacement measured by the transducer TL0_NCH2, which is installed on the construction discontinuity at ground level, on the North side (Fig. 5). It should be noticed that the measured opening, ranging between 0.12 mm and

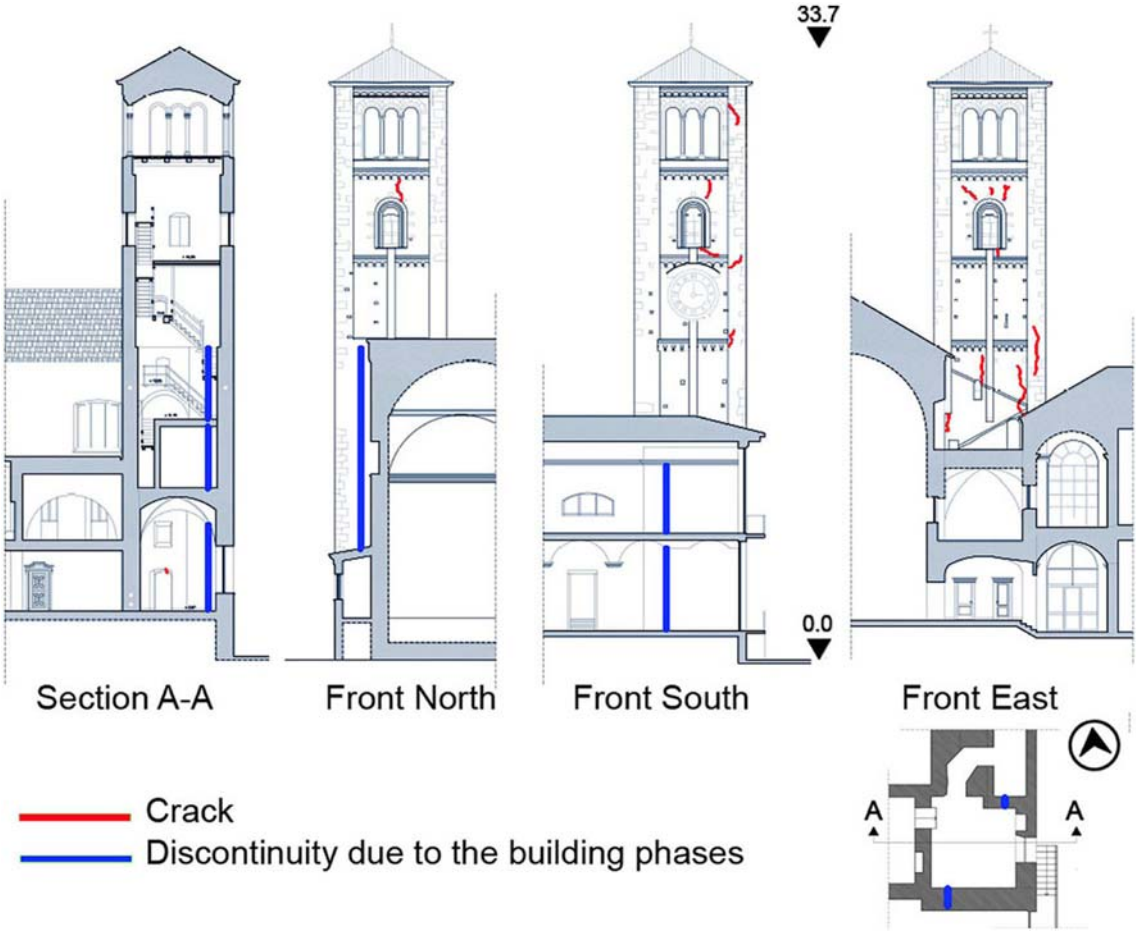

Fig. 3 Cross-section and fronts of the investigated tower

Fig. 4 Metallic tie-rod installed below the belfry (Level 2, West side)

+ 0.39 mm, seems to be largely dominated by thermal effects, so that possible settlements at the foundation level could have been almost negligible. As shown in Fig. 7a, the time variation of measured displacement and temperatures exhibit a regular trend, with periodic repetition of the crack opening measured in similar temperature conditions and inverse correlation between temperature and displacement. The correlation between the crack opening and the indoor temperature T_{0N} is better investi-gated in Fig. 7b and confirms that the irreversible com-ponent of the measured crack opening is practically negligible. Moreover, the inspection of Fig. 7b reveals an almost linear correlation until the indoor temperature T_{0N} does not exceed 20–22 °C; for higher temperatures, a clear stiffening effect is detected and likely associated with the closure of the gap between the walls of the church and the tower. It is further noticed that the nonlinear regression line shown in Fig. 7b exhibits an excellent fit of the measured data, with the coefficient of determination R^2 [18] being equal to 0.981.

As it is exemplified in Figs. 7a and 8a, all the main cracks tend to close with increased temperature, with the exception of the one denoted as TL2_SOCH2: Fig. 8b shows that the crack opening exhibits significant daily variation, with the displacement envelope closely follow-ing the evolution of indoor/outdoor temperature. This unusual trend is conceivably dependent on the structural effect exerted by the metallic tie-rod (Figs. 4, 6b) installed

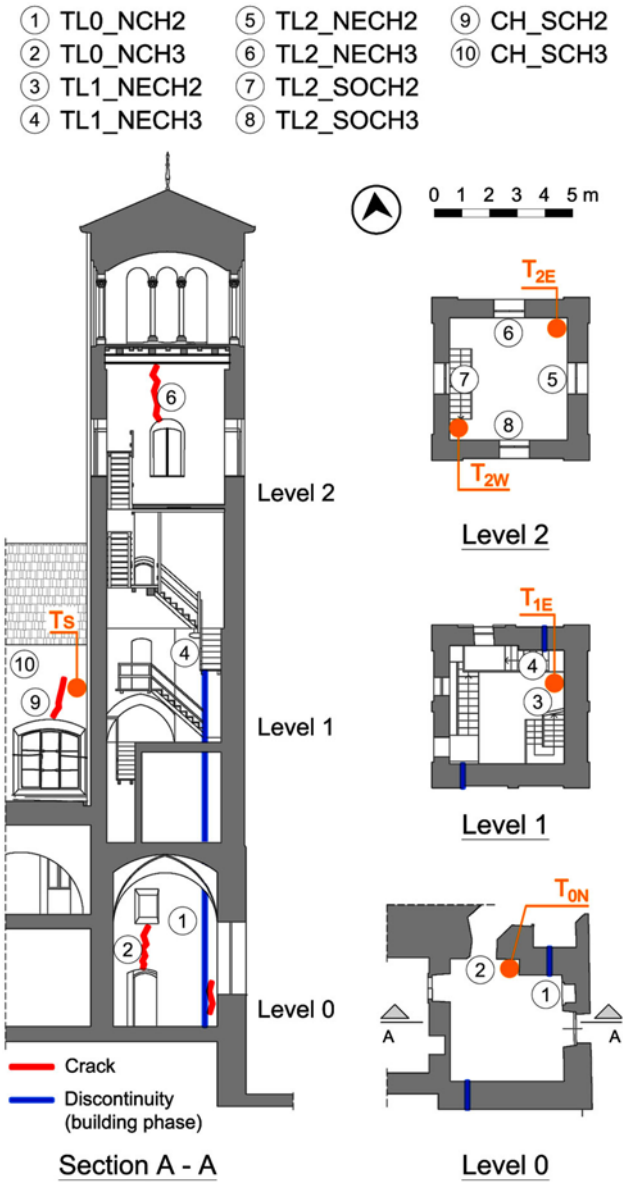

Fig. 5 General layout of the static monitoring system

above the crack and connecting the North and South load-bearing walls: as the temperature increases, the loss of tension in the tie-rod induces the opening of the cracks.

3 Dynamic characteristics of the bell-tower

Two series of ambient vibration tests (AVTs) were carried out on September–October 2015 [17].

The first AVT, performed on 23 September 2015, was mainly aimed at evaluating the baseline dynamic characteristics of the tower before the installation of a continuous dynamic monitoring system in the building. Ambient vibration data were recorded at a sampling frequency of

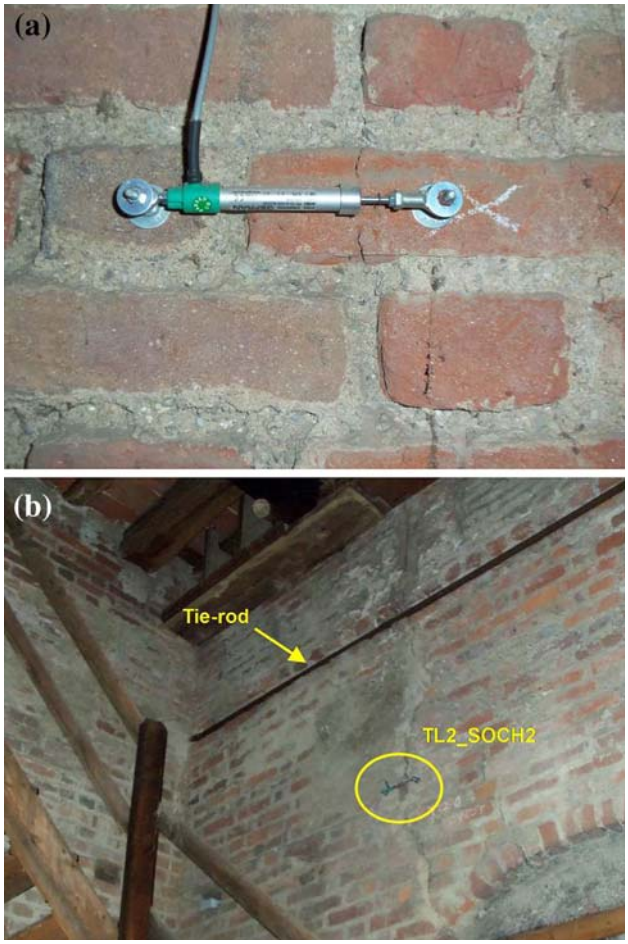

Fig. 6 **a** Displacement transducer on a crack; **b** displacement transducer TL2_SOCH2 installed on the main crack below the metallic tie-rod on West side

200 Hz using a multi-channel acquisition system with NI 9234 data acquisition modules (24-bit resolution, 102 dB dynamic range and anti-aliasing filters) and high-sensitivity WR 731A accelerometers (10 V/g sensitivity and ± 0.50 g peak acceleration). In order to improve the performance of the acquisition chain, each accelerometer was connected with a short cable (1 m) to a WR P31 power unit/amplifier, providing the constant current needed to power the accelerometer's internal amplifier, signal amplification and selective filtering. All the sensors were connected to the data acquisition system through two-conductor cables.

The accelerometers' layout adopted in the AVT is schematically shown in Fig. 9 and allows to identify both the bending modes in the N–S and E–W direction and the torsion modes.

The modal identification was performed using time windows of 3600 s and applying both the frequency domain decomposition (FDD) [19] and the covariance driven stochastic subspace identification (SSI-Cov) [20] methods. Although the level of ambient excitation that

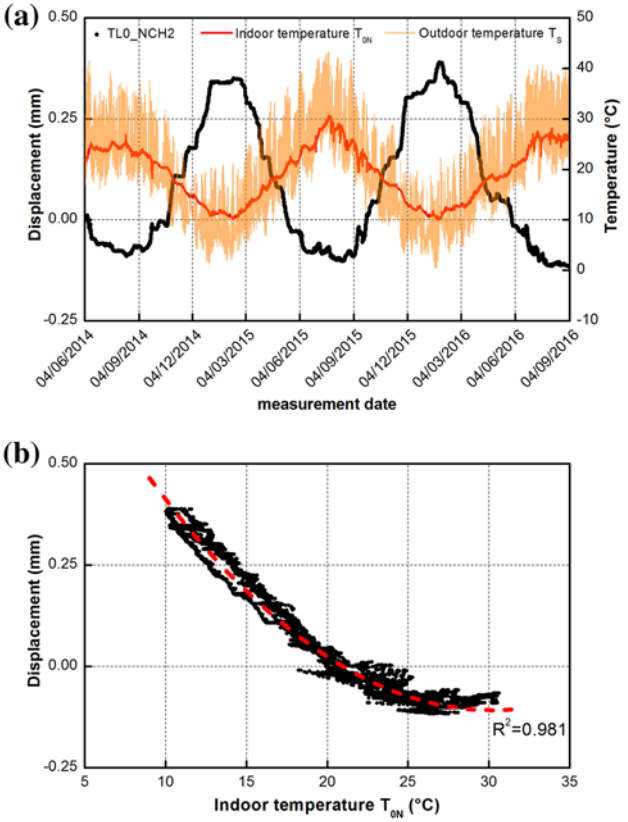

Fig. 7 **a** Time variation of displacement TL0_NCH2 (Level 0), indoor and outdoor temperature; **b** correlation between the displacement TL0_NCH2 and the indoor temperature

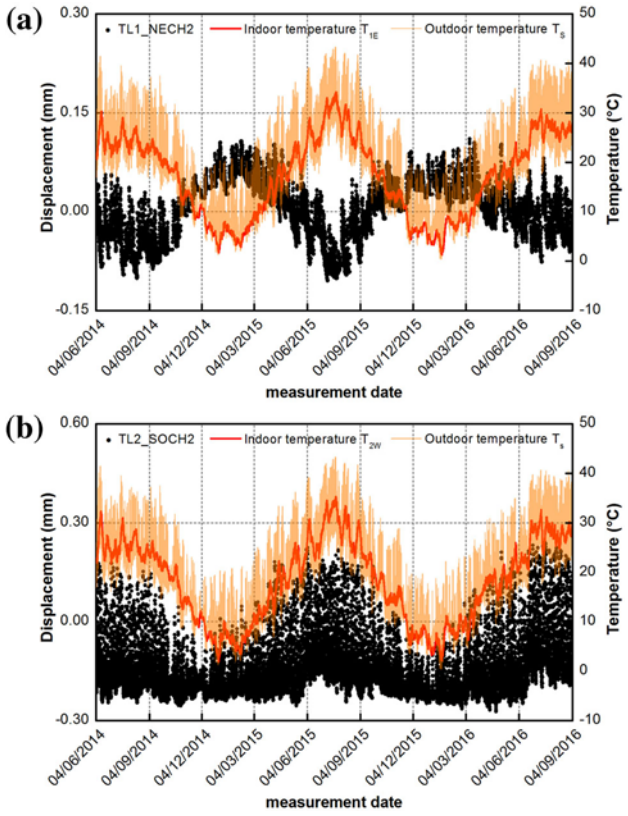

Fig. 8 **a** Time variation of displacement TL1_NCH2 (Level 1), indoor and outdoor temperature; **b** time variation of displacement TL2_SOCH2 (Level 2), indoor and outdoor temperature

existed during the tests was quite low, with the measured acceleration not exceeding 0.02 m/s^2, the application of the FDD and SSI-Cov techniques to the collected data allowed the identification of seven vibration modes in the frequency range 0–8 Hz. Table 1 summarizes the modal estimates provided by the two complementary FDD and SSI-Cov methods and the mode classification; more specifically, Table 1 compares the corresponding natural frequencies and scaled modal vectors through the frequency discrep-ancy $D_F = |(f_{SSI} - f_{FDD})/f_{SSI}|$ and the modal assurance criterion (MAC) [21]. Inspection of the correlation values listed in Table 1 highlights an excellent agreement between the two methods in terms of both natural frequencies and mode shapes.

The identified mode shapes are shown in Fig. 10 (SSI-Cov) and reveal distinctive dynamic characteristics of the bell-tower, that are conceivably related to the structural arrangement and construction sequence of the building. In more details, closely spaced modes with similar mode shapes were clearly identified, so that the sequence of identified modes turns out to be very different from the expected [8–14] regular series of two bending modes (one for each principal plane of the structure) and one torsion mode. The identified sequence of vibration modes (Fig. 10) consists of: (a) the fundamental mode ($f_{x1} = 1.92$ Hz, Fig. 10a), involving dominant bending in the E–W direc-tion; (b) two bending modes in the N–S direction, that are characterized by closely spaced natural frequencies ($f_{y1} = 2.01$ Hz and $f^*_{y1} = 2.37$ Hz) and very similar mode shapes (Figs. 10b, c); (c) another mode of dominant bending, again in the N–S direction ($f_{y2} = 4.14$ Hz, Fig. 10d); (d) two torsion modes ($f_{T1} = 4.55$ Hz and $f_{T2} = 5.25$ Hz) with very similar mode shapes (Figs. 10e, f); (e) the last mode ($f_{x2} = 7.53$ Hz, Fig. 10g), involving almost pure bending in the E–W direction.

Between 2 October 2015 and 9 October 2015, a second series of AVTs was performed by installing 4 WR-731A accelerometers at the Level 2 and continuously collecting the dynamic response of the tower for about 1 week at a sampling rate of 200 Hz [17]. It should be noticed that the instrumented level—although not optimal for the identification of all modes since the deflections of one mode (Fig. 10d) are negligible at this level—is the higher one suitable to the installation of a continuous dynamic moni-toring system. Since the second series of AVTs allowed to identify with high occurrence four vibration modes of the tower (i.e. the three lower bending modes and the torsion

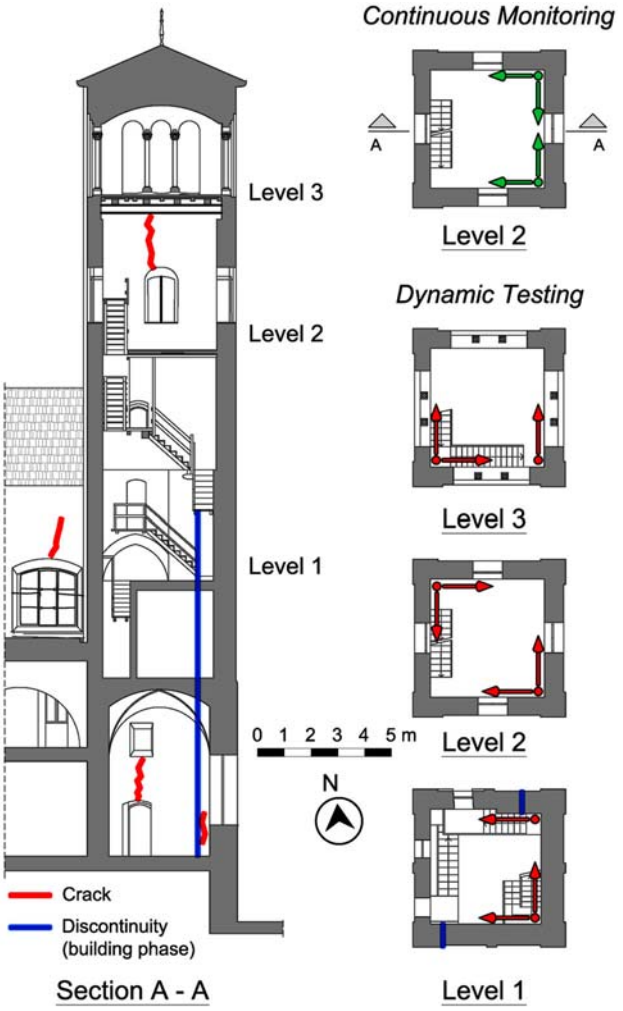

Fig. 9 Instrumented cross-sections and layout of the accelerometers during the preliminary dynamic tests (September 2015) and the continuous monitoring

mode f_{T2} of Fig. 10) and also considering the possibility of increasing the knowledge of the historic building through the combined use of static and dynamic monitoring, it was decided to permanently instrument the bell-tower with the same sensor layout (four accelerometers at Level 2) adopted in the second series of dynamic tests.

4 Dynamic monitoring hardware and shm methodology

4.1 Monitoring hardware and signal pre-processing

As previously pointed out, the tower was continuously instrumented for about 1 week with the main objective of evaluating the suitability of Level 2 to host the dynamic monitoring system. In this second series of AVTs, the performances of different sensing hardware were also compared with the ones of the WR-731A accelerometers, which were assumed as reference. Among the available sensors, well-known MEMS accelerometers (Kistler model 8330A3, 1.2 V/g sensitivity, ± 3.00 g peak acceleration, 1.3 μg resolution and 0.4 $\mu g/\sqrt{Hz}$ rms noise density) provided practically the same results of the reference sensors (in terms of both measured time histories and identified modal parameters) and were selected for the use in the continuous monitoring.

The continuous dynamic monitoring system is now active since 22 October 2015. The devices installed inside the bell-tower consisted of 4 MEMS accelerometers (Fig. 11), one Ethernet carrier with NI 9234 data acquisi-tion module and one local PC for the management of the continuous acquisition and the data storage. Data are recorded at 200 Hz and stored on the local PC in separate files of 60 min.

The collected acceleration data are processed through a series of tools developed in the LabVIEW environment and comprising the following tasks [22]: (a) creation of a database with the original data (in compact format) for later developments; (b) signal pre-processing with de-trending and despiking of the raw data; (c) automatic detection and extraction of the time series associated with swinging of bells and numerical integration to estimate velocity time histories; (d) creation, for each 1-h dataset, of one time window containing only the ambient vibration response; (e) statistical analysis of the previously extracted data; (f) low-pass filtering and decimation of the each "bell-free" dataset and creation of a second database of files (in binary or text format) for the application of the

Table 1 Dynamic characteristics of the bell-tower identified from OMA

Mode n.	Mode identifier	f_{SSI} (Hz)	f_{FDD} (Hz)	D_f (%)	MAC
1	f_{x1} (E–W bending)	1.916	1.924	0.42	0.9997
2	f_{y1} (N–S bending)	2.011	2.012	0.05	0.9989
3	f^*_{y1} (N–S bending)	2.367	2.363	0.17	1.0000
4	f_{y2} (N–S bending)	4.139	4.160	0.51	0.9748
5	f_{T1} (torsion)	4.554	4.570	0.35	0.9733
6	f_{T2} (torsion)	5.248	5.176	1.37	0.9883
7	f_{x2} (E–W bending)	7.528	7.539	0.15	0.9783

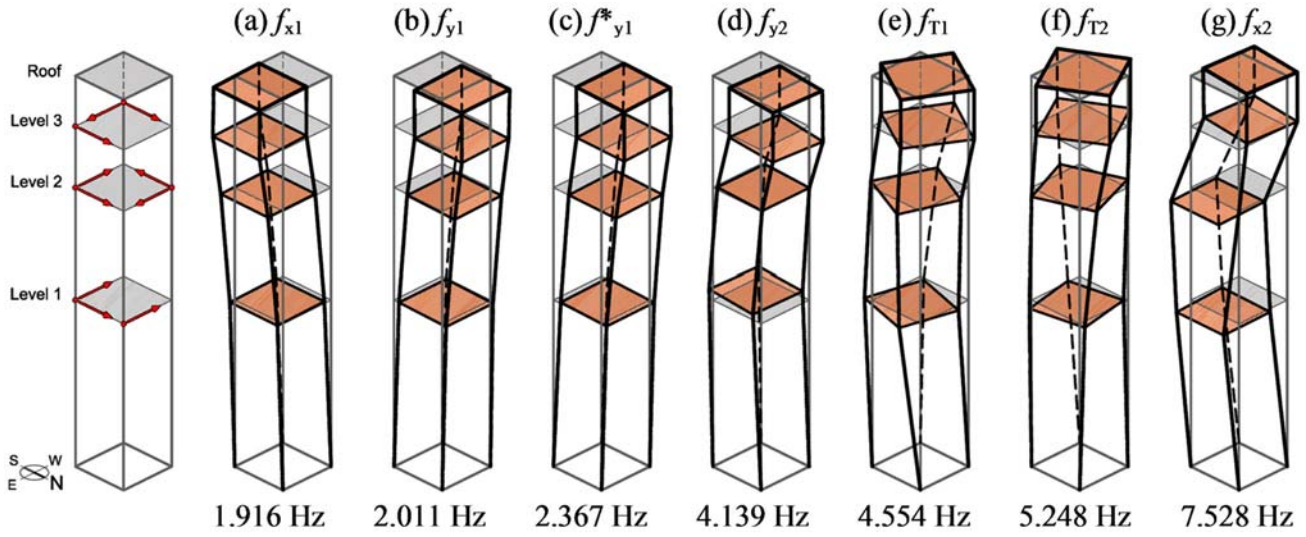

Fig. 10 Identified vibration modes of the bell-tower (AVT 23 September 2015, SSI-Cov)

Fig. 11 MEMS accelerometers (Kistler, model 8330A3) adopted in the continuous monitoring

modal identification tools [6]. During this last step, each set of "bell-free" time histories (low-pass-filtered using 7th order Butterworth filter with cut-off frequency of 12.5 Hz and decimated to reduce the sampling frequency from 200 to 25 Hz) was reduced to a uniform time window of 3000 s.

4.2 Automated modal identification

The modal parameters of the bell-tower were extracted from each 3000-s acceleration dataset using a fully automated procedure, based on the SSI-Cov algorithm [20] and developed in a previous study [6].

SSI identification procedures [20] are based on the discrete-time stochastic state-space form of the dynamics of a linear-time-invariant system under unknown excitation:

$$x_{k+1} = Ax_k + w_k \quad (1)$$

$$y_k = Cx_k + v_k \quad (2)$$

where $x_k \in \Re^n$ is the discrete-time state vector (containing displacements and velocities describing the state of the system at time instant $t_k = k\Delta t$), $\boldsymbol{y}_k \in \Re^m$ is the output vector, $\boldsymbol{w}_k$ is the process noise, $\boldsymbol{v}_k$ is the measurement noise, $A \in \Re^{n \times n}$ is the discrete state matrix (dependent on the mass, stiffness and damping properties of the structure), $C \in \Re^{m \times n}$ is the discrete output matrix (which maps the state vector into the measured outputs), n is the system order and m represents the number of outputs.

Once matrices $\boldsymbol{A}$, $\boldsymbol{C}$ of different order n are identified, $n/2$ sets of modal parameters are extracted from a model of order n: natural frequencies and damping ratios are calculated from the eigenvalues of $\boldsymbol{A}$, whereas the mode shapes are evaluated from the product of $\boldsymbol{C}$ and the eigenvectors of $\boldsymbol{A}$.

The automated procedure [6] involves the two main steps of modal parameters estimation and modal tracking:

1. The estimation phase is performed through an automatic interpretation of stabilization diagrams, based on the sensitivity of frequency and mode shape to the model order variation. To increase the efficiency of this step, spurious poles are eliminated by checking the corresponding damping ratio and modal complexity value. For each dataset, the modes which share similar frequencies and mode shapes are clustered together. For each cluster, a set of representative modal parameters (i.e. natural frequency, damping and mode shape) is estimated.
2. The automated modal tracking, aimed at providing the frequency evolution for each mode over the monitoring

period, is based on frequency and MAC variation with respect to a pre-selected list of baseline modes.

For the details on the automated modal identification, the interested reader is referred to [6]. As it is common to SSI-based approaches, the adopted procedure [6] needs some input parameters, whose setting was carried out through a preliminary manual analysis of the data collected before the installation of the monitoring system. In the present application: (a) the time lag parameter i needed to fill the ($mi \times mi$) block Toeplitz matrix [20] (that is decomposed to obtain the matrices $\boldsymbol{A}$, $\boldsymbol{C}$) was set equal to 75; (b) the order of the model has been varied from 20 to 120; (c) the maximum allowable damping ratio and modal complexity index [6], adopted in the noise modes elimination step, were set equal to 10% and 0.20, respectively.

4.3 Modelling the environmental effects and health assessment methodology

Although the present paper is mainly aimed at demonstrating the challenging behaviour exhibited by the investigated bell-tower and the importance of continuous monitoring to enhance the knowledge of a historic building, the description of the adopted SHM strategy is concisely completed in this subsection. As it is more extensively reported in [4, 12] and [14], the vibration-based health assessment involves the combined use of automated operational modal analysis, procedures to mitigate the environmental effects on identified natural frequencies and multivariate statistical tools to detect the occurrence of abnormal structural changes.

Among the different procedures reported in the literature (see e.g. [4, 8, 12, 14]) to remove the environmental effects from identified frequency data, the well-known multiple linear regression (MLR, see e.g. [23]) will be adopted. This choice is motivated by the availability of multiple temperature measurements, as well as by the possibility of accounting for possible nonlinear dependence on temperature. In fact, even if the response variable d_k (for example, the r-th modal frequency) at current time k is expressed as a second-order surface model of predictor variables $T_{j,k}$ and $T_{j,k}^2$ at time k (for example, the measured temperatures and their square values):

$$d_k = \beta_0 + \beta_1 T_{1,k} + \cdots + \beta_p T_{p,k} + \beta_{p+1} T_{1,k}^2 + \cdots + \beta_{2p} T_{p,k}^2 + \varepsilon_k \tag{3}$$

the resulting model (3), which is linear in the parameters weighting the predictors (i.e. the βs), is still a MLR model.

The general MLR model, regardless the shape of the response surface it generates, can be expressed in matrix form as:

$$d = Z\beta + \varepsilon \tag{4}$$

where $d \in \Re^N$ is the vector containing N observations d_k of the dependent variable, $\beta \in \Re^{p+1}$ is the vector formed by the $(p + 1)$ parameters weighting the contribution of the input parameters, $\varepsilon \in \Re^N$ is the vector of the random errors, and $Z \in \Re^{N \times (p+1)}$ is the matrix appropriately gathering the measured values of the predictors.

It is worth mentioning that in the general framework of a dynamic monitoring project, different input candidates might be considered in MLR models (4), such as temperature, humidity, wind speed, traffic loads on bridges [4, 8, 14]. In the present application, only the measured temperatures have been considered as input or predictor variables for each natural frequency.

In order to properly describe the influence of changing environmental conditions, the data used to estimate the parameters of the MLR models should be collected over an appropriate period of time, denoted as training or reference period and including a statistically representative sample of environmental conditions.

After one MLR model (4) has been established for each natural frequency, the occurrence of anomalies not observed during the training period might be detected from residual error vectors $\varepsilon_j = d_j - Z_j\beta_j \quad (j = 1, 2, \ldots, M$ where M is the number of automatically identified modal frequencies), using the statistical tools defined as "control charts". A control chart (see e.g. [23] and [4, 12, 13] for background theory and practical applications, respectively) typically consists of a plot where the variation in time of a feature (i.e. the residual errors) is represented along with a user-defined variation limit. The designated control limit, computed from the experimental samples collected when the process is supposed to be in control (training period), allows to check if the fluctuations of the monitored feature are associated with the normal response. Any observation laying outside the control limit has to be considered the result of unusual sources of variability (e.g. the occurrence of damage).

It is further noticed that the SHM methodology outlined in this subsection should allow [11–13] to detect the onset of non-reversible structural anomalies, whereas the development of a numerical model of the tower is needed to localize possible damage and estimate its severity [24]. Hence, the development of a finite element model of the bell-tower, including the interaction with the church, is ongoing with the twofold objective of:

(a) Better understanding the structural motivations leading to the presence of the two closely spaced modes

with eigenfrequencies f_{y1} and f^*_{y1}. In fact, it is expected [25] that an appropriate numerical model is capable of indicating whether the deflections associated with the closely spaced modes involve only the bell-tower or the overall complex tower + church. This key information, in turn, could allow to estimate the effects of the complex interaction between the tower and the church determined by the common load-bearing walls, the presence of vertical gaps between the walls of the church and the tower, and the crack pattern observed on East and West load-bearing walls of the tower. It is worth mentioning that the information provided by the response to the swinging of bells might be very useful in the model validation phase.

(b) Localizing the possible onset of non-reversible structural anomalies and assessing the damage extent and severity (for example, through the procedure outlined in [24]).

5 Continuous dynamic monitoring: results

This section summarizes the main results of the continuous dynamic monitoring in the first year after the installation (i.e. between 22 October 2015 and 21 October 2016). During this time interval, about 8000 datasets were collected and automatically processed to identify the modal parameters.

Figure 12 presents the evolution of the identified modal frequencies, whereas the relevant statistics are summarized in Table 2 through the mean value (f_{ave}), the standard deviation (σ_f), and the extreme values (f_{min}, f_{max}) of each natural frequency.

The results summarized in Fig. 12 and Table 2 allow the following comments:

1. Notwithstanding the low level of the ambient excita-tion, four normal modes were identified with high occurrence and accuracy.
2. The identification rate is higher for the lower 3 modes, ranging from 86.0% for mode f_{y1} to 99.3% for mode f^*_{y1}, and decreases to 77.6% for torsion mode f_{T2}.
3. The natural frequency of modes f_{x1} and f_{T2} (Fig. 12) exhibits significant increase in Spring and Summer period. This trend suggests that these modal frequencies are strongly affected by the temperature and—as it had to be expected from previous studies [8–14] on masonry towers—increase with increased temperature.
4. On the contrary, the natural frequency of modes f_{y1} and f^*_{y1} exhibits very limited variation, with the standard deviation being equal to 0.009 and 0.015 Hz, respectively. For those modes, the trend of modal frequency to increase with increased temperature is conceivably balanced by the loss of tension in the metallic tie-rod placed on the West side and connecting the North and South load-bearing walls of the bell-tower (Figs. 4, 6b). The loss of tension in the tie-rod, in turn, is also confirmed by the time evolution of the observed

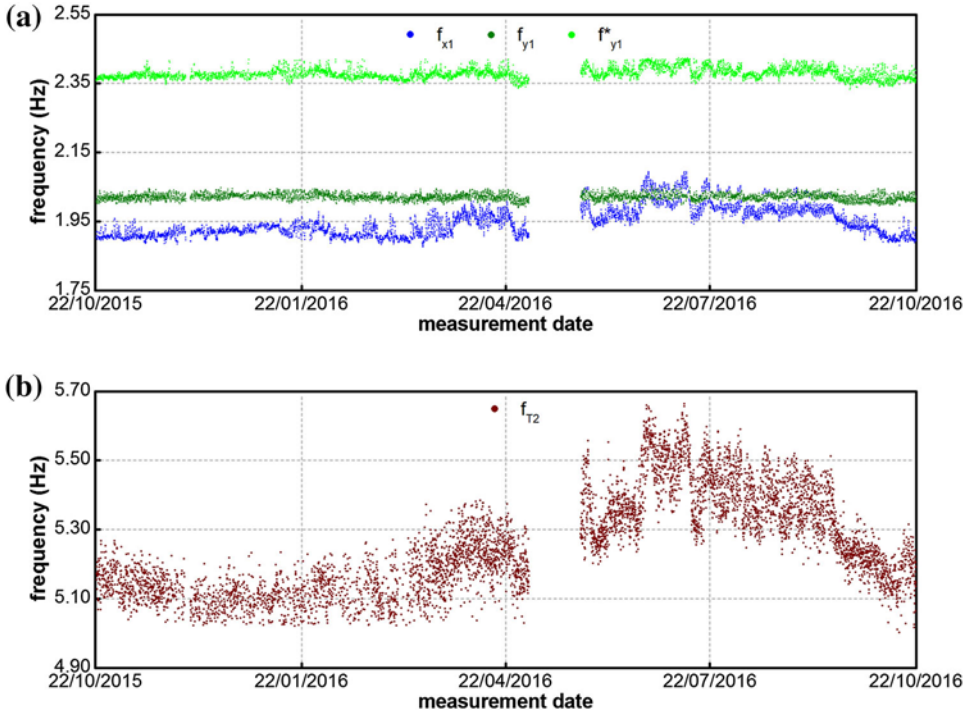

Fig. 12 Automatically identified natural frequencies of the bell-tower versus time: **a** modes f_{x1}, f_{y1} and f^*_{y1}; **b** mode f_{T2}

Table 2 Statistics of the natural frequencies identified (SSI-Cov) from 22 October 2015 to 21 October 2016

Mode id.	f_{ave} (Hz)	f_f (Hz)	f_{min} (Hz)	f_{max} (Hz)
f_{x1}	1.946	0.041	1.876	2.094
f_{y1}	2.020	0.009	1.990	2.053
f^*_{y1}	2.379	0.015	2.333	2.423
f_{T2}	5.265	0.141	5.001	5.663

displacement on the main crack of the West side (Fig. 8b).

5. As shown in Fig. 12, the natural frequencies of the two lower modes f_{x1} and f_{y1} exhibit crossing in Summer months. To the authors' knowledge, such a crossing phenomenon has not been observed before on masonry towers and clearly depends on the different effect exerted by the temperature on the natural frequency of the two lower modes. In addition, the mode shape of both modes f_{x1} and f_{y1} tends to hybridize when crossing occurs: in other words, the two modes—which are usually associated with pure bending in orthogonal planes, as illustrated in Figs. 10a, b—tend to involve biaxial bending in both the main E–W and N–S directions when the natural frequencies become very close to each other. It is further noticed that this hybridization, suggesting the occurrence of something similar to mode veering (see e.g. [26, 27]), is more significantly detected for mode f_{y1}.

It is worth mentioning that also the first torsion mode f_{T1} was often automatically identified. The results are not shown herein because the modal identification process revealed some unexpected issues for this mode: by inspecting the first singular value line (i.e. which is the mode indication function of FDD technique) of the recorded data, it is possible to detect the presence of spurious harmonics close to the natural frequency f_{T1}. The impossibility of eliminating such perturbing elements, conceivably produced by some active machineries present in the close neighbourhood of the building, undermines the quality of the frequency estimates.

In order to better investigate the effects of changing temperature on the natural frequencies, Fig. 13 shows the hourly averaged value of the measured temperatures in the monitoring period from 22 October 2015 to 21 October 2016. Table 3 summarizes the correlation coefficients [18] between the environmental data during the same period.

Both Fig. 13 and Table 3 indicate that a large degree of correlation exists between all temperature data, with the measurements T_{1E}, T_{2E} and T_{2W} being almost perfectly correlated and characterized by correlation coefficients very close to unity. Hence, using only one of those temperatures in establishing the MLR model of each modal frequency is suggested.

The correlation coefficients between natural frequencies and temperatures are reported in Table 4, whereas the identified natural frequencies have been plotted versus the outdoor temperature T_S in Figs. 14 and 15, along with the best fit line and the coefficient of determination R^2.

Figure 14 refers to modes f_{x1} and f_{T2} and confirms that the frequency of those modes increases with increased temperature, with the same information being provided by the correlation coefficients of Table 4. Moreover, Fig. 14 shows that—although the overall frequency–temperature correlations are almost linear and characterized by high values of the coefficient of determination R^2—slight nonlinearity is detected in the low temperature range ($T_S \leq 10$ °C) for the frequency of mode f_{x1}.

Figure 15 refers to closely spaced and similar modes f_{y1} and f^*_{y1} and confirms the very low effect of the changing environment on the frequency of these modes, already demonstrated by the frequency tracking (Fig. 12a).

6 Conclusions

The importance of continuous monitoring to enhance the knowledge and assist the preservation of a challenging historic bell-tower has been addressed in the paper. The investigated Heritage tower, adjacent to the church of "Santa Maria del Carrobiolo" in Monza (Italy), is especially interesting as it exhibits a weak structural arrangement, with two sides of the bell-tower being directly supported by the load-bearing walls of the apse and South aisle of the neighbouring church. In addition, the East and West fronts of the tower exhibit major cracks and other important cracks are visible on all sides at the level below the belfry, with the opening of a deep crack on the West side being opposed by the presence of one metallic tie-rod.

The monitoring hardware installed in the bell-tower includes a network of 10 displacement transducers, mounted on the main cracks and integrated by five temperature sensors, as well as four accelerometers. The static monitoring system is active since June 2014, whereas the dynamic monitoring began on late October 2015.

The results of static monitoring allowed to highlight the absence of abnormal increase in the cracks' opening, which is dominated by the thermal effects: as it has to be expected, all the main cracks tend to close with increased temperature, with the exception of the one placed on the West side below the metallic tie-rod.

The dynamic characteristics of the bell-tower and the results of 1-year dynamic monitoring allow to significantly deepen the knowledge of the global structural behaviour of the bell-tower and reveal some unique aspects, which are

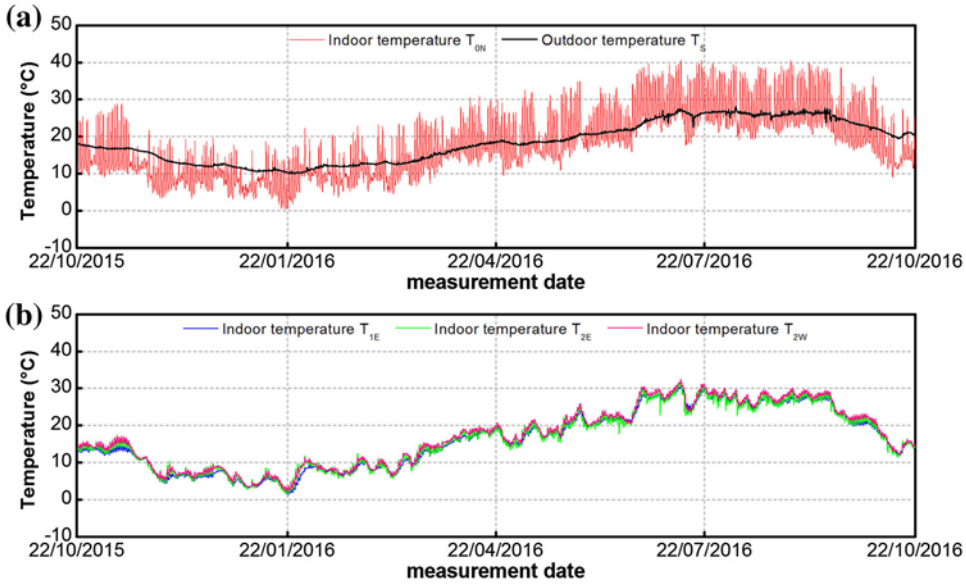

Fig. 13 Variation in time of measured temperatures: **a** T_{0N} and T_S; **b** T_{1E}, T_{2E} and T_{2W}

Table 3 Correlation coefficients between the measured temperatures (from 22 October 2015 to 21 October 2016)

	T_{0N}	T_{1E}	T_{2E}	T_{2W}	T_S
T_{0N}	1.000	0.967	0.957	0.960	0.837
T_{1E}		1.000	0.995	0.997	0.873
T_{2E}			1.000	0.998	0.900
T_{2W}				1.000	0.885
T_S					1.000

Table 4 Correlation coefficients between natural frequencies and temperatures (from 22 October 2015 to 21 October 2016)

	T_{0N}	T_{1E}	T_{2E}	T_{2W}	T_S
f_{x1}	0.663	0.768	0.789	0.778	0.803
f_{y1}	− 0.067	− 0.004	− 0.007	0.002	− 0.221
f^*_{y1}	0.293	0.402	0.416	0.415	0.292
f_{T2}	0.791	0.866	0.876	0.869	0.821

conceivably related to the structural arrangement of the building and to the observed crack pattern:

1. Closely spaced modes with similar mode shapes were clearly identified, so that the modal characteristics of the bell-tower significantly differ from those obtained in past experimental studies of similar structures [8–14]. Since the closely spaced and similar modes are the lower bending modes in the N–S plane, this distinctive behaviour is possibly related to the complex interaction between the bell-tower and the church, determined by the common load-bearing walls.

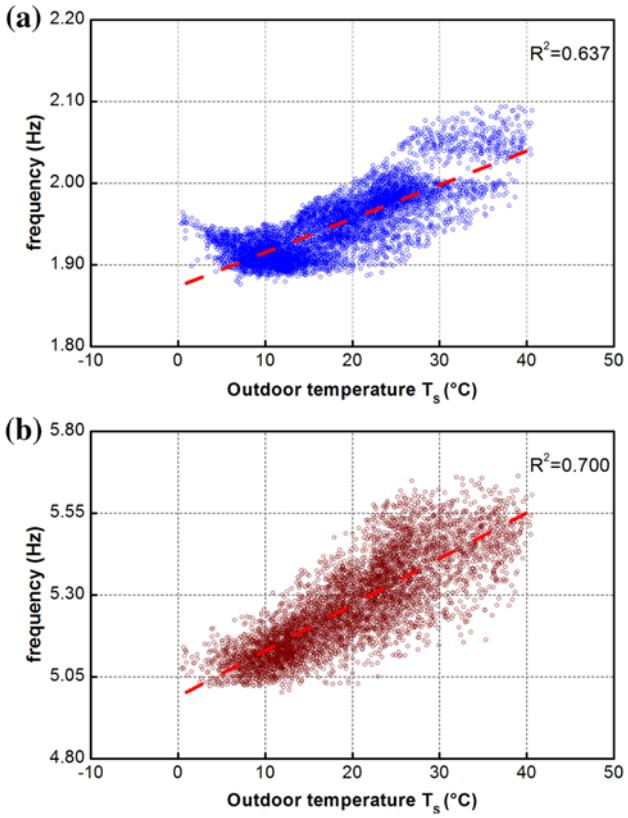

Fig. 14 Correlation between outdoor temperature T_S and natural frequencies f_{x1} **a** and f_{T2} **b**

2. The application of state-of-art tools for automated operational modal analysis, within the continuous dynamic monitoring of the investigated tower, allows accurate estimate and tracking of four natural frequencies. The automatically identified frequencies involve

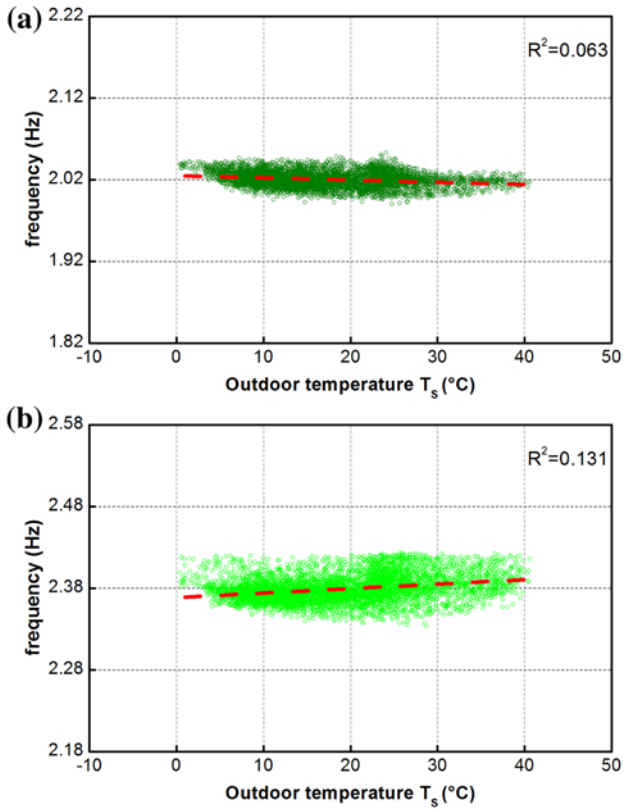

Fig. 15 Correlation between outdoor temperature T_S and natural frequencies f_{y1} **a** and f^*_{y1} **b**

dominant bending in the E–W direction (f_{x1}), dominant bending in the N–S direction (closely spaced modes f_{y1} and f^*_{y1}) and torsion (f_{T2}).

3. The temperature turned out to be a dominant driver of daily fluctuation of the natural frequencies of modes f_{x1} and f_{T2}, with those frequencies increasing with increased temperature. On the contrary, the frequency of the closely spaced and similar modes f_{y1} and f^*_{y1} are slightly affected by the environmental changes, as the temperature effects on the masonry material and the metallic tie-rod placed on the West side tend to balance.
4. The natural frequencies of the two lower modes f_{x1} and f_{y1} exhibit crossing as the temperature increases. This behaviour, not observed so far in masonry towers, is associated with the different effect exerted by the changing temperature on the natural frequency of the two lower modes. In addition, the hybridization of the shape of both modes f_{x1} and f_{y1} (with the hybridization being more significant for the latter mode) occurs when the natural frequencies are close to each other, so that the resulting phenomenon seems more similar to mode veering [26, 27] than to simple frequency crossing.

As a final remark, the results of static and dynamic monitoring allowed to highlight some distinctive and unique structural behaviour, which will be of utmost importance for both the numerical modelling and the preservation of the tower.

Acknowledgements The pre-diagnostic survey was partially supported by Fondazione CARIPLO, project "Concio d'Argilla". The community of the Barnabite Order in Monza, Father R. Cagliani, Eng. L. Sorteni and Arch. L. Valsasnini are gratefully acknowledged for the assistance during the field tests and the management/maintenance of the monitoring systems.

References

1. Luzi L, Pacor F, Ameri G, Puglia R, Burrato P, Massa M, Augliera P, Franceschina G, Lovati S, Castro R (2013) Overview on the strong-motion data recorded during the May–June 2012 Emilia seismic sequence. Seismol Res Lett 84(4):629–644. https://doi.org/10.1785/0220120154
2. ReLUIS-INGV Workgroup (2016) Preliminary study on strong motion data of the 2016 central Italy seismic sequence V6. http://www.reluis.it. Accessed 1 June 2017
3. Bartoli G, Betti M, Marra AM, Monchetti S (2017) Semi-empirical formulations for estimating the main frequency of slender masonry towers. J Perform Constr Facil ASCE 31(4):04017025. https://doi.org/10.1061/(ASCE)CF.1943-5509.0001017
4. Magalhães F, Cunha À, Caetano E (2012) Vibration based structural health monitoring of an arch bridge: from automated OMA to damage detection. Mech Syst Signal Pr 28:212–228. https://doi.org/10.1016/j.ymssp.2011.06.011
5. Reynders E, Houbrechts J, De Roeck G (2012) Fully automated (operational) modal analysis. Mech Syst Signal Pr 29:228–250. https://doi.org/10.1016/j.ymssp.2012.01.007
6. Cabboi A, Magalhães F, Gentile C, Cunha A (2017) Automated modal identification and tracking: application to an iron arch bridge. Struct Control Health Monit 24(1):e1854. https://doi.org/10.1002/stc.1854
7. Cardoso R, Cury A, Barbosa F (2017) A robust methodology for modal parameters estimation applied to SHM. Mech Syst Signal Pr 95:24–41. https://doi.org/10.1016/j.ymssp.2017.03.021
8. Ramos LF, Marques L, Lourenço PB, DeRoeck G, Campos-Costa A, Roque J (2010) Monitoring historical masonry structures with operational modal analysis: two case studies. Mech Syst Signal Pr 24(5):1291–1305. https://doi.org/10.1016/j.ymssp.2010.01.011
9. Cabboi A (2013) Automatic operational modal analysis: challenges and application to historic structures and infrastructures. Ph.D. Thesis, University of Cagliari, Italy
10. Cantieni R (2014) One-year monitoring of a historic bell tower. In: Proceedings of the 9th international conference on structural dynamics (EURODYN 2014), Porto, Portugal, pp. 1493–1500
11. Guidobaldi M (2016) Vibration-based structural health monitoring for historic masonry towers. Ph.D. Thesis, Politecnico di Milano, Italy
12. Gentile C, Guidobaldi M, Saisi A (2016) One-year dynamic monitoring of a historic tower: damage detection under changing environment. Meccanica 51:2873–2889. https://doi.org/10.1007/s11012-016-0482-3
13. Ubertini F, Cavalagli N, Kita A, Comanducci G (2017) Assessment of a monumental masonry bell-tower after 2016 Central Italy seismic sequence by long-term SHM. Bull Earthquake Eng. https://doi.org/10.1007/s10518-017-0222-7

14. Ubertini F, Comanducci G, Cavalagli N, Pisello AL, Materazzi AL, Cotana F (2017) Environmental effects on natural frequencies of the San Pietro bell tower in Perugia, Italy and their removal for structural performance assessment. Mech Syst Signal Pr 82:307–322. https://doi.org/10.1016/j.ymssp.2016.05.025
15. Sohn H (2007) Effects of environmental and operational variability on structural health monitoring. Philos Trans R Soc A 365:539–560. https://doi.org/10.1098/rsta.2006.1935
16. Magnani Pucci P, Colombo M, Marsili G (1997) The church of Santa Maria di Carrobiolo (in Italian), SPA Tipografica Sociale
17. Saisi A, Gentile C, Ruccolo A (2016) Pre-diagnostic prompt investigation and static monitoring of a historic bell-tower. Constr Build Mater 122:833–844. https://doi.org/10.1016/j.conbuildmat.2016.04.016
18. Draper NR, Smith H (1998) Applied Regression Analysis, 3rd edn. Wiley Interscience, Hoboken
19. Brincker R, Zhang L, Andersen P (2001) Modal identification of output-only systems using frequency domain decomposition. Smart Mater Struct 10:441–445. https://doi.org/10.1088/0964-1726/10/3/303
20. Peeters B, De Roeck G (1999) Reference-based stochastic subspace identification for output-only modal analysis. Mech Syst Signal Proc 13(6):855–878. https://doi.org/10.1006/mssp.1999.1249
21. Allemang RJ, Brown DL (1982) A correlation coefficient for modal vector analysis. In: Proceedings of the 1st international modal analysis conference (IMAC-I), Orlando, USA
22. Saisi A, Busatta F, Gentile C, Ruccolo A (2016) Monitoring cultural heritage buildings: the Santa Maria del Carrobiolo bell-tower in Monza, Italy. In: Proceedings 6th international conference on structural engineering, mechanics and computation, Cape Town, South Africa, pp. 1902–1907
23. Montgomery D (1997) Introduction to statistical quality control. John Wiley & Sons Inc., Hoboken
24. Cabboi A, Gentile C, Saisi A (2017) From continuous vibration monitoring to FEM-based damage assessment: application on a stone-masonry tower. Constr Build Mater 156:252–265. https://doi.org/10.1016/j.conbuildmat.2017.08.160
25. Morassi A, Polentarutti F (2011) Dynamic testing and structural identification of the Hypo Bank office complex. II: identification. J Struct Eng ASCE 137(12):1540–1552. https://doi.org/10.1061/(ASCE)ST.1943-541X.0000399
26. Benedettini F, Zulli D, Alaggio R (2009) Frequency-veering and mode hybridization in arch bridges. In: Proceedings of the 27th international modal analysis conference (IMAC-XXVII), Orlando, USA
27. Giannini O, Sestieri A (2016) Experimental characterization of veering crossing and lock-in in simple mechanical systems. Mech Syst Signal Proc 72–73:846–864. https://doi.org/10.1016/j.ymssp.2015.11.012